Materials and Corrosion **2010**, 61, No. 4

DOI: 10.1002/maco.200905333

Electrochemical and surface analytical studies of synergistic effect of phosphonate, Zn^{2+} and ascorbate in corrosion control of carbon steel

B. V. Appa Rao* and S. Srinivasa Rao

Synergistic inhibition of corrosion of carbon steel in low chloride environment using ascorbate as a synergist along with 2-phosphonobutane-1,2,4-tricarboxylic acid (PBTC) and Zn^{2+} is presented. The synergistic effect of ascorbate has been established from the present studies. In the presence of ascorbate, lower concentrations of PBTC and Zn^{2+} are sufficient in order to obtain good inhibition, thus making this formulation more environmentally friendly. Potentiodynamic polarisation studies inferred that this mixture functions as a mixed inhibitor, predominantly cathodic. Impedance studies revealed that an immersion period of 24 h is necessary for the formation of the protective film, with a very high charge transfer resistance. The film is stable even at 60 °C in the presence of the inhibitor in the corrosive environment. The surface analysis by X-ray photoelectron spectroscopy (XPS) showed the presence of iron, oxygen, phosphorus, carbon and zinc in the protective film. The XPS spectra inferred the presence of oxides/hydroxides of iron(III), $Zn(OH)_2$ and [Zn(II)–PBTC–ascorbate] complex in the surface film. This inference was further supported by the reflection absorption Fourier transform infrared spectrum of the surface film. A plausible mechanism of corrosion inhibition has been proposed.

1 Introduction

It is well known that phosphonate/Zn^{2+} mixtures are prominent inhibitors to control corrosion of carbon steel in cooling water systems. Synergistic effect existing between phosphonic acids and zinc ions on the inhibition of corrosion of carbon steel has been studied by several researchers [1–7]. The reports pointing to synergistic action of phosphonates and Zn^{2+} explained that the inhibiting action is due to the formation of protective films on the metal surface [2]. It was also reported that phosphonates act anodically and form complexes with metal ions while Zn^{2+} ions act cathodically and form $Zn(OH)_2$ resulting in the synergistic corrosion inhibition [8]. However, these highly effective phosphonate/Zn^{2+} formulations require high levels of both Zn^{2+} and phosphonate. But, the disposal of zinc salts in wastewaters at higher levels has become unacceptable. The tolerated content of zinc in water is restricted to about 2 mg/dm^3 [9]. Owing to these strict environmental restrictions on industrial wastewater disposal, research has been progressed in the direction to minimise the concentration of Zn^{2+} in the inhibitor formulations. An interesting method to handle this task is to add another non-toxic component of either organic or inorganic nature, which can synergistically act along with phosphonate and Zn^{2+} and bring about effective corrosion inhibition at relatively lower concentrations of zinc ions. The formulations are referred to as ternary inhibitor systems. A few of such formulations were reported in the literature [10–12].

In this background, a new ternary inhibitor formulation with relatively low concentrations of both phosphonate and Zn^{2+} in the presence of an organic compound has been proposed in the present study. The selected phosphonic acid and the organic compound are 2-phosphonobutane-1,2,4-tricarboxylic acid (PBTC) and ascorbic acid, respectively. PBTC consists of one phosphonic acid group and three carboxylic acid groups. The oral and dermal toxicity of PBTC, as tested in rats have been found to be very low [13]. The ecological risk for aquatic organisms has been reported to be the lowest for PBTC among several phosphonates studied [13]. Therefore, this compound is environmentally friendly. *Ashcraft* et al. [14]. studied the inhibitive film formed on carbon steel in the presence of PBTC. *Bohnsack* et al. [15] inferred that phosphonocarboxylic acids, like PBTC, are able to prevent precipitation of ferric hydroxide. Ascorbic acid is well known to be an environmentally friendly compound.

B. V. Appa Rao, S. Srinivasa Rao
Department of Chemistry, National Institute of Technology (NITW), Warangal 506 004, Andhra Pradesh (India)
E-mail: boyapativapparao@rediffmail.com

Ascorbate ion contains five hydroxyl groups and one carboxyl group and has the complexing ability with metal ions [16, 17]. The main objective of the present study is to investigate the electrochemical and surface analytical aspects of the synergistic action of the selected compounds, namely PBTC, Zn^{2+} and ascorbate in the corrosion control of carbon steel in chloride and nearly neutral aqueous environment. For all these studies, 200 ppm of sodium chloride solution has been chosen as control because of the following reason: the water used in the cooling water systems is generally either demineralised water or unpolluted surface water. In either case, the aggressiveness of the water will never exceed that of 200 ppm of sodium chloride.

2 Experimental

2.1 Materials

For all the studies, the specimens taken from a single sheet of carbon steel of the following composition were chosen: C, 0.1–0.2%; P, 0.03–0.08%; S, 0.02–0.03%; Mn, 0.4–0.5% and the rest iron. Prior to the tests, the specimens were polished to mirror finish with 1/0, 2/0, 3/0 and 4/0 emery polishing papers, respectively, washed with distilled water, degreased with acetone and dried. For gravimetric measurements, the polished specimens of the dimensions, 3.5 cm × 1.5 cm × 0.2 cm, were used while for other studies, the dimensions of the specimens are 1.0 cm × 1.0 cm × 0.1 cm. PBTC ($C_7H_{11}O_9P$), zinc sulphate ($ZnSO_4{\cdot}7H_2O$), ascorbic acid ($C_6H_8O_6$) and other reagents were analytical grade chemicals. Molecular structures of PBTC and ascorbic acid are shown in Figs. 1 and 2, respectively. All the solutions were prepared by using triple distilled non-deaerated water. pH values of the solutions were adjusted by using 0.01 N sodium hydroxide and 0.01 N sulphuric acid solutions. An aqueous solution consisting of 200 ppm of sodium chloride has been used as the control throughout the studies.

2.2 Gravimetric measurements

In all the gravimetric experiments, the polished specimens were weighed and immersed in duplicate, in 100 mL control solution in the absence and presence of inhibitor formulations of different concentrations, for a period of 7 days. Then the specimens were reweighed after washing, degreasing and drying. During the studies, only those results were taken into consideration, in which the difference in the weight-loss of the two specimens immersed in the same solution did not exceed 0.1 mg. Accuracy in weighing up to 0.01 mg and in surface area measured up to 0.1 cm^2, as recommended by ASTM G31, was followed [18]. The immersion period of 7 days was fixed in view of the considerable magnitude of the corrosion rate (CR) obtained in the absence of any inhibitor after this immersion period. The immersion period was maintained accurately up to 0.1 h in view of the lengthy immersion time of 168 h. Under these conditions of accuracy, the relative standard error in CR determinations is of the order of 2% or less for an immersion time of 168 h [19].

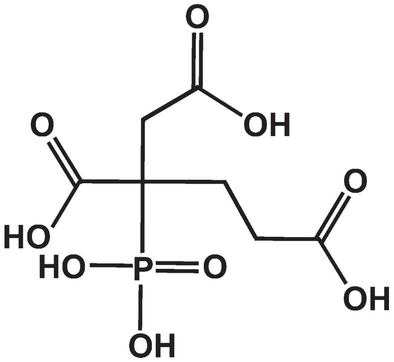

Figure 1. Molecular structure of PBTC

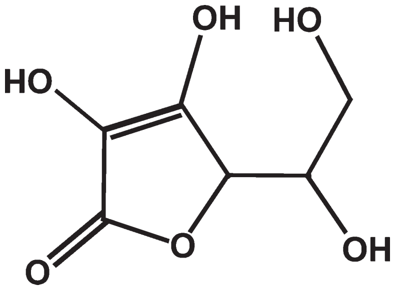

Figure 2. Molecular structure of ascorbic acid

CRs of carbon steel in the absence and presence of various inhibitor formulations are expressed in mmpy. Inhibition efficiencies (IE_w) of the inhibitor formulations were calculated by using the formula

$$IE_w\ (\%) = 100\ [(CR)_o - (CR)_I]/(CR)_o \quad (1)$$

where $(CR)_o$ and $(CR)_I$ are the CRs in the absence and presence of inhibitor, respectively.

The gravimetric studies were first carried out on the binary system containing PBTC (30–50 ppm) and Zn^{2+} (30–100 ppm). The results of these studies were used to fix the concentration ranges of PBTC and Zn^{2+} in the ternary inhibitor formulations. Gravimetric studies of the ternary formulations containing PBTC (20–40 ppm), Zn^{2+} (10–20 ppm) and ascorbate (10–200 ppm) were carried out at pH 7. The influence of pH on inhibition efficiency of the effective inhibitor formulations was also studied in the pH range, 4–9. Gravimetric experiments were also conducted with the specimens after the formation of the protective film in the ternary inhibitor formulation, in order to decide the required minimum dosage of each of the components for maintenance of the protective film in the chosen corrosive environment.

2.3 Electrochemical studies

Both the potentiodynamic polarisation studies and electrochemical impedance spectroscopic (EIS) studies were carried out using Electrochemical Workstation Model IM6e, Zahner-Elektrik, GmbH, Germany and the experimental data were analysed by using the Thales software. The measurements were conducted in a conventional three-electrode cylindrical glass cell with platinum electrode as auxiliary electrode and Ag/AgCl as reference electrode. The working electrode was carbon steel embedded in epoxy resin of polytetrafluoroethylene so that the flat surface of 1 cm^2 was the only surface exposed to the electrolyte. The three-electrode set up was immersed in control solution of volume 500 mL both in the absence and presence of various inhibitor formulations and allowed to attain a stable open circuit potential (OCP). The pH values of the solutions were adjusted to 7.0 and the solutions were unstirred during the experiments.

Polarisation curves were recorded in the potential range of −1000 to +200 mV with a resolution of 2 mV. The curves were recorded in the dynamic scan mode with a scan rate of 2 mV/s in the current range of −20 to +20 mA. The ohmic drop compensation has been made during the studies. The corrosion potential (E_{corr}), corrosion current (I_{corr}) and anodic Tafel slope (β_a) and cathodic Tafel slope (β_c) were obtained by extrapolation of anodic and cathodic regions of the Tafel plots. The inhibition efficiency (IE_p) values were calculated from I_{corr} values using the equation [20]

$$IE_p\ (\%) = [1 - (I'_{corr}/I_{corr})] \times 100 \qquad (2)$$

where I_{corr} and I'_{corr} are the corrosion current densities in case of control and inhibited solutions, respectively.

Electrochemical impedance spectra in the form of Nyquist plots were recorded at OCP in the frequency range from 60 kHz to 10 mHz with 4–10 steps per decade. A sine wave, with 10 mV amplitude, was used to perturb the system. The impedance parameters, viz. charge transfer resistance (R_{ct}) and constant phase element (CPE) and CPE exponent (n) were obtained from the Nyquist plots. The inhibition efficiencies (IE_i) were calculated using the equation

$$IE_i\ (\%) = 100\ [1 - (R_{ct}/R'_{ct})] \qquad (3)$$

where R_{ct} and R'_{ct} are the charge transfer resistance values in the absence and presence of the inhibitor, respectively. In order to study the effect of immersion period, the three-electrode set up was kept undisturbed for 24 h and impedance spectra were recorded at various immersion periods, namely 1, 6, 12 and 24 h. In order to conduct the tests at various temperatures, the working electrode was immersed in the environment for 24 h at 30 °C to ensure the formation of the protective film. The Nyquist plots were then recorded at higher temperatures up to 60 °C. The temperature of the cell was controlled by using thermostat arrangement, with an accuracy of ±0.1 °C.

2.4 X-ray photoelectron spectroscopy (XPS)

XPS measurements of the surface films were carried out with Kratos analytical photoelectron spectrometer model AXIS 165 with monochromated Al Kα X-ray source (1486.6 eV) operated at 100 W. Both the survey spectra and deconvolution spectra were recorded at four spots on each specimen. The average of the four measurements is reported. The spectra were collected at an electron take-off angle of 90°. Analyser pass energy was 80 eV, with a step of 1 eV. Deconvolution spectra were recorded with analyser pass energy of 80 eV, with a step of 0.1 eV for the elements of interest namely Fe 2p, O 1s, P 2p, C 1s and Zn 2p. Binding energies for the deconvolution spectra were corrected individually for each measurement set, based on a value of 285.0 eV for the C–C component of C 1s.

2.5 Fourier transform infrared (FTIR) spectroscopy

FTIR spectra were recorded using FTIR spectrophotometer from Thermo Electron Corporation, USA, model Nexus 670 with a resolving power of 0.125 cm^{-1}. The detector is temperature stabilised DTGS (KBr window) and liquid nitrogen cooled MCT-A and the beam splitter is XT-KBr. FTIR spectra of pure PBTC and pure ascorbic acid were recorded using KBr pellet method. The reflection absorption FTIR spectra of the surface films were recorded in the wave number range of 4000–400 cm^{-1}. The measurements were made at a grazing angle of 85°.

3 Results and discussion

3.1 Gravimetric studies

The results of gravimetric studies using the binary inhibitor formulation, PBTC–Zn^{2+}, are shown in Fig. 3. These results indicate that PBTC alone in the concentration range of 30–50 ppm aggravates corrosion of carbon steel. As expected, addition of Zn^{2+} to PBTC offered good corrosion inhibition at optimum concentrations of each of the components, due to synergistic effect. For example, at the concentration of 30 ppm of PBTC equivalent to 1.1×10^{-4} M, the inhibition efficiency increased with the increase in concentration of Zn^{2+} in the mixture, reached a maximum of 81% at a concentration of 30 ppm of Zn^{2+}, equivalent to 4.6×10^{-4} M and then reduced with a further increase in the concentration of Zn^{2+}. The highest inhibition efficiency corresponds to a molar ratio of [Zn^{2+}]/[PBTC] as 4.2:1. At the higher concentrations of PBTC such as 40 ppm (1.5×10^{-4} M) and 50 ppm (1.9×10^{-4} M), the same trend of variation of inhibition efficiency with the increase in concentration of Zn^{2+} in the mixture is observed. The highest inhibition efficiencies of 98% correspond to a molar ratio of 4.2:1 ([Zn^{2+}]/[PBTC]) at 1.5×10^{-4} M PBTC and to a molar ratio of 3.3:1 at 1.9×10^{-4} M PBTC. At lower or higher molar

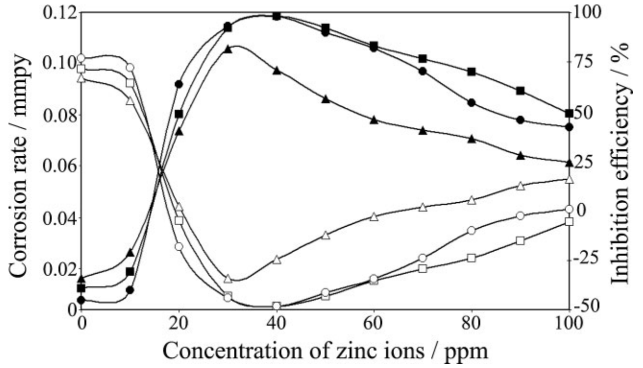

Figure 3. Corrosion rate (CR) of carbon steel and inhibition efficiency (IE) of the binary inhibitor formulation, PBTC–Zn^{2+} as a function of concentration of Zn^{2+} at various concentrations of PBTC at pH 7 [PBTC] = 30 ppm: CR —△—, IE —▲—; [PBTC] = 40 ppm: CR —□—, IE —■—; [PBTC] = 50 ppm: CR —○—, IE —●—

ratios of [Zn^{2+}]/[PBTC] than those mentioned above, the inhibition efficiencies are found to be less. These results indicate that the synergistic effect operating between PBTC and Zn^{2+} is the highest at a given molar ratio of [Zn^{2+}]/[PBTC] in solution. However, to afford higher inhibition efficiency >95%, the minimum required concentrations of PBTC and Zn^{2+}, respectively, are 1.5×10^{-4} and 6.2×10^{-4} M. It is worth mentioning the molar ratios corresponding to highest inhibition efficiencies in case of other phosphonate–Zn^{2+} combinations reported in the literature. For Zn(II)–HEDP system, at the molar ratio of [Zn^{2+}]/[HEDP] as 3, and at the concentration of 3×10^{-4} M HEDP the highest inhibition efficiency was reported [7]. In the case of aminotris (methylenephosphonic acid) (AMP), at the molar ratio of [Zn^{2+}]/[AMP] as 1, the highest inhibition efficiency was obtained at the comparable concentrations. *Deluchat* et al. [21] determined the complexation constants ($\log K_s$) of AMP and HEDP with Zn^{2+}, each of them being at the concentration of 2×10^{-3} M, in aqueous 0.1 M KNO_3 solution. They reported the highest value of $\log K_s$ for the complex between Zn(II) and completely deprotonated ligand. The authors also reported an increase in complexed cation level with an increase in pH from 5 to 8 and a decrease at pH 9. This trend is more evident in case of HEDP, with $\log K_s$ value of 10.3, which is much less than the $\log K_s$ value of 16.3 for AMP. This trend must be true in case of Zn(II)–PBTC combination also as the $\log K_s$ value of PBTC is only 8.3. At low pH values ≤5, the protonation of ligand is more, which is not favourable for the complex formation and at pH values ≥9, there is OH^- ion interference in complexation of PBTC with Zn(II). In the present study, the concentrations of Zn^{2+} and PBTC corresponding to the highest inhibition efficiency are 6.2×10^{-4} and 1.5×10^{-4} M, respectively. That means much higher concentration of Zn^{2+} in comparison to that of PBTC is required to afford the highest efficiency of inhibition. This can be explained as follows:

The complexation equilibrium between Zn^{2+} ions and PBTC is as follows:

$$Zn^{2+} + L^{5-} \rightleftarrows [Zn - L]^{3-} \text{ complexed species}$$

where L^{5-} indicates the completely deprotonated ligand of PBTC. The value of $\log K_s$ is 8.3

$$K_s = [Zn - L]^{3-}/[Zn^{2+}]\,[L^{5-}] \qquad (4)$$

When the concentration of Zn^{2+} is much higher, the equilibrium is shifted towards right and the concentration of the [Zn–PBTC]$^{3-}$ complex increases. Sufficient concentration of this complex is necessary to get attached to the metal surface at anodic sites. Secondly, there will be enough concentration of free zinc ions at the molar ratio of [Zn^{2+}]/[PBTC] as 4.2. It is also necessary that free zinc ions from solution diffuse to the metal surface and precipitate optimum amount of zinc hydroxide at the cathodic sites. For Zn(II)–HEDP system, at the molar ratio of [Zn^{2+}]/[HEDP] as 3, the highest inhibition efficiency was reported at the concentration of HEDP as 3×10^{-4} M [7]. This is because the $\log K_s$ value of HEDP is somewhat higher than that of PBTC. In the case of AMP, at the molar ratio of [Zn^{2+}]/[AMP] as 1, the highest inhibition efficiency was obtained at the comparable concentrations. The $\log K_s$ of AMP is as high as 16.3 [21]. These observations lead to a generalisation that at a particular molar ratio of [Zn^{2+}]/[phosphonic acid] and at an optimum concentration of the phosphonic acid, the highest inhibition efficiency is obtained. The higher the $\log K_s$ value of [Zn^{2+}–phosphonic acid]$^{x-}$ complex, the lower is the molar ratio of [Zn^{2+}]/[phosphonic acid] required for the highest inhibition efficiency.

Ascorbic acid exists as monoanion in the pH range, 4–9 and the chelate-type coordination of ascorbate with metal ions has been reported [22]. When ascorbate is added as another additive to the mixture of PBTC and Zn^{2+} at relatively low concentrations of each, CR of carbon steel is found to be reduced significantly. Hence, the ternary inhibitor formulations containing 20–40 ppm of PBTC and 10–20 ppm of Zn^{2+} are considered along with ascorbate (10–200 ppm). The results of CRs are shown in Fig. 4. None of the formulations containing 10 or 15 ppm of Zn^{2+} showed inhibition efficiency >52% even when the concentrations of PBTC and ascorbate are increased to 40 and 200 ppm, respectively. In order to achieve an inhibition efficiency >95%, the required minimum concentrations of PBTC and Zn^{2+} are 20 ppm each only corresponding to 0.75×10^{-4} and 3.1×10^{-4} M, respectively, in the presence of ascorbate. While the binary system consisting of 20 ppm each of PBTC and Zn^{2+} showed an inhibition efficiency of only 22%, the ternary inhibitor system containing 25 ppm of ascorbate and 20 ppm each of PBTC and Zn^{2+}, afforded an inhibition efficiency of 98%. The synergistic effect of ascorbate in the ternary system is established by this result. However, at very high concentrations of ascorbate such as 150 and 200 ppm, the inhibition efficiency is reduced to 21 and 4%, respectively. It can be observed from Fig. 4 that in case of all the ternary inhibitor formulations, as the concentration of ascorbate is increased, the CR decreases, reaches a minimum at an optimum concentration of ascorbate and then increases. Thus, in case of the ternary inhibitor formulation also, the mixture containing optimum concentrations of each of the components gives the highest inhibition efficiency. In other words, optimum amounts of each of the three components must be available in the solution, so that each one of them plays its own synergistic role in

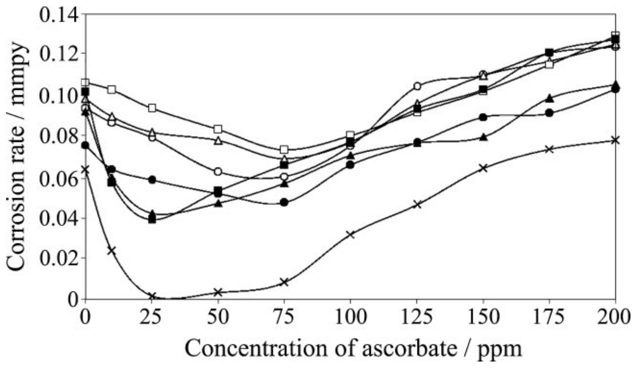

Figure 4. CR of carbon steel as a function of concentration of ascorbate, added to various combinations of PBTC and Zn^{2+} at pH 7: —○—, PBTC (20 ppm) + Zn^{2+} (10 ppm); —△—, PBTC (30 ppm) + Zn^{2+} (10 ppm); —□—, PBTC (40 ppm) + Zn^{2+} (10 ppm); —●—, PBTC (20 ppm) + Zn^{2+} (15 ppm); —▲—, PBTC (30 ppm) + Zn^{2+} (15 ppm); —■—, PBTC (40 ppm) + Zn^{2+} (15 ppm); —×—, PBTC (20 ppm) + Zn^{2+} (20 ppm)

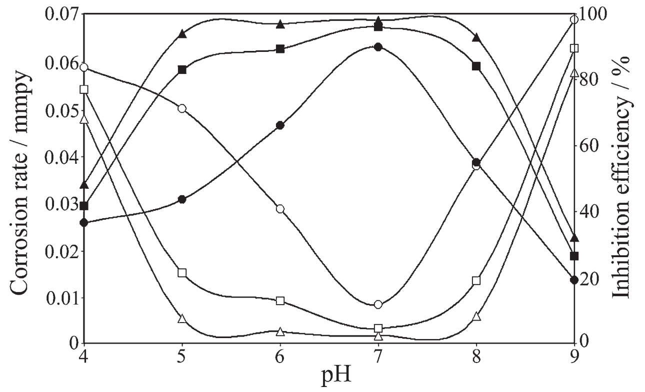

Figure 5. CR of carbon steel and IE of the ternary inhibitor formulation, PBTC (20 ppm) + Zn^{2+} (20 ppm) + ascorbate, as a function of pH at various concentrations of ascorbate 25 ppm: CR —△—, IE —▲—; 50 ppm: CR —□—, IE —■—; 75 ppm: CR —○—, IE —●—

the formation of protective film covering the entire metal surface. It may be mentioned here that the molar ratios of PBTC/Zn^{2+}/ascorbate are 1.0:4.2:2.0 and 1.0:4.2:4.0 to exhibit excellent synergism with an efficiency >95%.

The influence of pH on CRs of carbon steel in the presence of the ternary inhibitor system and the inhibition efficiencies of the inhibitor namely, PBTC (20 ppm) + Zn^{2+} (20 ppm) + ascorbate (25–75 ppm), in the pH range of 4.0–9.0 are shown in Fig. 5. The highest inhibition efficiency could be obtained by the formulation containing PBTC (20 ppm) + Zn^{2+} (20 ppm) + ascorbate (25 ppm) in the pH range of 5–8. But when the pH is decreased from 5.0 to 4.0, the inhibition efficiency is reduced to 48% and when the pH is increased from 8.0 to 9.0, the inhibition efficiency is reduced to 32.5%. The reasons for decrease in inhibition efficiency in more alkaline and more acidic environments are explained under the mechanistic aspects. Once, the protective film is formed on the metal surface by using the ternary inhibitor system consisting of PBTC (20 ppm), Zn^{2+} (20 ppm) and ascorbate (25 ppm), the concentrations of each of these components in the inhibitor could be even less in order to maintain the protective film. The results of gravimetric studies carried out in order to determine the minimum concentrations of the formulation for maintenance of the protective film are shown in Table 1. These results show that the inhibitor mixture containing only 10 ppm of PBTC, 10 ppm of Zn^{2+} and 15 ppm of ascorbate could maintain the protective film. The molar ratio of PBTC/Zn^{2+}/ascorbate in the maintenance dosage is 1.0:4.2:2.3.

Table 1. Results of gravimetric studies of the inhibitor formulations for maintenance of the protective film

Inhibitor formulation for maintenance of the film (ppm)			Corrosion rate (mmpy)	Inhibition efficiency (%)
[PBTC]	[Zn^{2+}]	[Ascorbate]		
–	–	–	0.08108	–
20	20	25	0.00167	97.93
20	15	25	0.00469	94.21
20	10	25	0.00576	92.89
20	5	25	0.06311	22.16
15	10	25	0.00645	92.03
10	10	25	0.00683	91.58
5	10	25	0.07086	12.60
10	10	20	0.00701	91.35
10	10	15	0.00719	91.12
10	10	10	0.07165	11.62
10	10	5	0.08038	0.85

3.2 Potentiodynamic polarisation studies

The potentiodynamic polarisation curves of carbon steel electrode in 200 ppm NaCl solution at pH 7 in the absence and presence of various inhibitor combinations are shown in Figs. 6 and 7. The Tafel parameters derived from these curves and the inhibition efficiencies are listed in Table 2. The corrosion potential (E_{corr}) in case of the control is −323.4 mV *versus* Ag/AgCl and the corresponding corrosion current density (I_{corr}) is 13.00 $\mu A/cm^2$. PBTC alone shifts the E_{corr} value to more anodic side. In the presence of PBTC alone, a slight increase in anodic and cathodic current densities is observed in the potential range of −0.15 to −0.50 V. Beyond this range, the anodic and cathodic current densities are slightly reduced. I_{corr} value is reduced only to a small extent in the presence of PBTC alone. The shift in anodic Tafel slope (β_a) is greater than the shift in cathodic Tafel slope (β_c) in the presence of PBTC alone. According to the literature reports [8, 23], phosphonates in general are anodic inhibitors. When zinc ions alone are considered, the cathodic current density values are slightly reduced while the anodic current densities are increased. The cathodic reaction is controlled by the formation of zinc hydroxide at cathodic sites. The corrosion potential is shifted to cathodic side and the shift in cathodic Tafel slope is greater. Contrary to the result obtained in case of PBTC, zinc ions

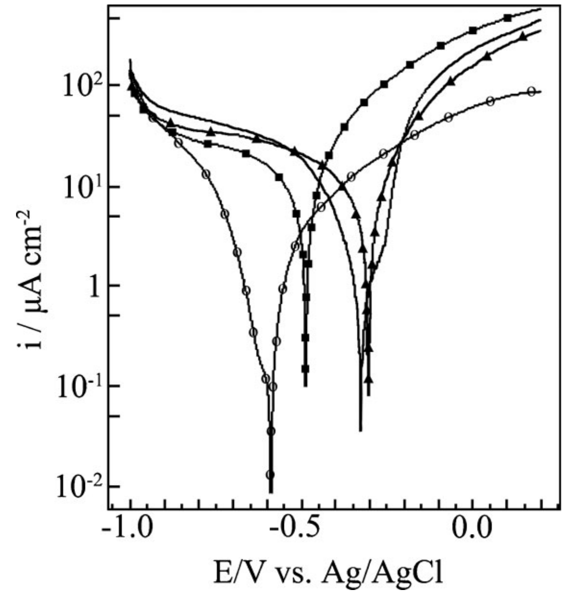

Figure 6. Potentiodynamic polarisation curves for carbon steel in various aqueous environments: ▬, NaCl (200 ppm); —▲—, NaCl (200 ppm) + PBTC (40 ppm); —■—, NaCl (200 ppm) + Zn^{2+} (40 ppm); —○—, NaCl (200 ppm) + PBTC (40 ppm) + Zn^{2+} (40 ppm)

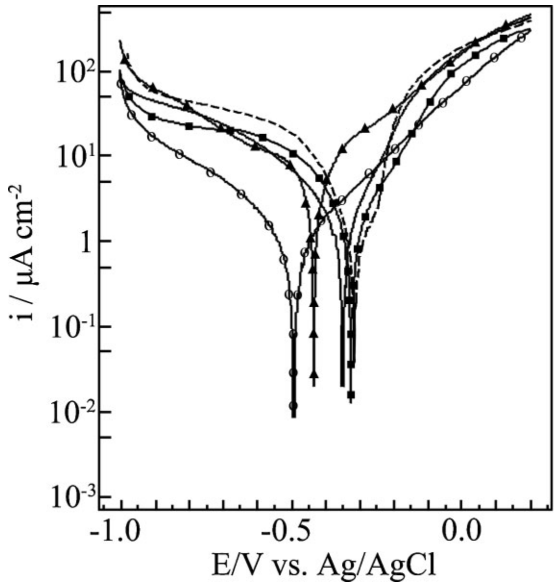

Figure 7. Potentiodynamic polarisation curves for carbon steel in 200 ppm NaCl in the presence of different combinations of the inhibitor: ▬ ▬, NaCl (200 ppm); ▬, PBTC (20 ppm) + Zn^{2+} (20 ppm); —▲—, PBTC (20 ppm) + ascorbate (25 ppm); —■—, Zn^{2+} (20 ppm) + ascorbate (25 ppm); —○—, PBTC (20 ppm) + Zn^{2+} (20 ppm) + ascorbate (25 ppm)

increased the rate of corrosion as inferred by increase in corrosion current density. Such an increase in CR in the presence of zinc ions alone was also reported in the literature [24]. From the polarisation curves shown in Fig. 6, it is clear that the combination of PBTC (40 ppm) and Zn^{2+} (40 ppm) significantly decreased both the anodic and cathodic current density values when compared to the control. It is thus evident that this formulation acts as an effective mixed type inhibitor. There is a tremendous shift of corrosion potential to more cathodic side and the shift in cathodic Tafel slope is greater than the shift in anodic Tafel slope. The corrosion current is significantly decreased to 1.14 μA/cm^2, corresponding to an inhibition efficiency of 91.23%. When the concentrations of both PBTC and Zn^{2+} are reduced to 20 ppm each, this binary formulation also showed similar trends in the shifts of E_{corr}, β_a and β_c. But the inhibition efficiency is only 65.92%. The other possible binary combinations namely PBTC (20 ppm) + ascorbate (25 ppm) and Zn^{2+} (20 ppm) + ascorbate (25 ppm) also shifted the corrosion potential to more cathodic side and decreased the corrosion current values. But none of these formulations afforded an inhibition efficiency greater than 58%. When 25 ppm of ascorbate is added to the control, the E_{corr} is slightly shifted to anodic side (curve not shown). Both the anodic and cathodic current densities are slightly reduced in the presence of ascorbate. Thus, it affects, though to a small extent, both the anodic and cathodic reactions. The corrosion current is reduced to some extent. The difference in the shifts of β_a and β_c is only 5 mV/dec. *Ferreira* et al. [25] studied the inhibitor effect of ascorbic acid on the corrosion of mild steel and inferred that it acts on both anodic and cathodic reactions. It is interesting to note that the ternary formulation containing PBTC (20 ppm), Zn^{2+} (20 ppm) and ascorbate (25 ppm) drastically decreased the I_{corr} value to 0.83 μA/cm^2, corresponding to an inhibition efficiency of 93.62%. This result is in agreement with the inhibition efficiency obtained from gravimetric studies. This result clearly infers the synergistic action of PBTC, Zn^{2+} and ascorbate in corrosion control of carbon steel. In the presence of ternary inhibitor formulation, both the cathodic and anodic current density values are significantly reduced. However, the decrease in cathodic current density is much higher. The corrosion potential is shifted to an extent of about 167 mV in the cathodic direction. It may also be noted that the shift in the cathodic Tafel slope is much higher than the shift in the anodic slope. All these results indicate that the ternary inhibitor formulation retards both the anodic dissolution of carbon steel and oxygen reduction at cathodic sites in the corrosion inhibition process. Nevertheless, the effect on cathodic reaction is more pronounced. Similar phosphonate-based formulations were reported to be mixed inhibitors in the literature [8, 26, 27].

3.3 Electrochemical impedance studies

Nyquist plots for carbon steel immersed in 200 ppm of NaCl solution at pH 7 in the absence and presence of various formulations are shown in Figs. 8 and 9. In case of the control as well as in the presence of various formulations, i.e. individual components, possible binary combinations and the ternary inhibitor formulation, the Nyquist plots are found to be depressed semicircles instead of ideal semicircles. This kind of phenomenon is called dispersing effect [28]. When the complex plane impedance contains a depressed semicircle with centre below the real axis, which is characteristic for solid electrodes, it is often

Table 2. Tafel parameters for carbon steel in 200 ppm NaCl environment in the absence and presence of inhibitor formulations

Concentration (ppm)			Tafel parameters				Inhibition efficiency, IE_p (%)
PBTC	Zn^{2+}	Ascorbate	E_{corr} (mV) *vs.* Ag/AgCl	I_{corr} (μA/cm^2)	β_a (mV/dec)	β_c (mV/dec)	
0	0	0	−323.4	13.00	228	794	–
40	0	0	−303.7	7.43	151	750	42.85
0	40	0	−494.9	16.23	306	642	−24.85
40	40	0	−592.3	1.14	170	184	91.23
20	20	0	−350.0	4.43	197	487	65.92
20	0	25	−436.6	6.57	322	569	49.46
0	20	25	−327.8	5.44	218	373	58.15
20	20	25	−490.9	0.83	253	243	93.62

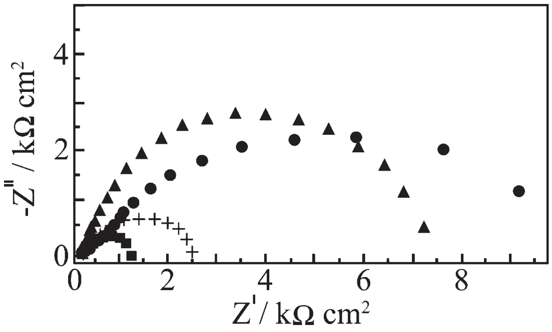

Figure 8. Nyquist plots for carbon steel in various aqueous environments: +, NaCl (200 ppm); ▲, NaCl (200 ppm) + PBTC (40 ppm); ■, NaCl (200 ppm) + Zn^{2+} (40 ppm); ●, NaCl (200 ppm) + PBTC (40 ppm) + Zn^{2+} (40 ppm)

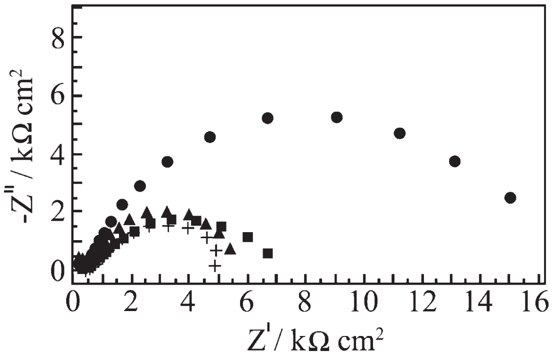

Figure 9. Nyquist plots for carbon steel in 200 ppm NaCl in the presence of different combinations of the inhibitor: +, PBTC (20 ppm) + Zn^{2+} (20 ppm); ▲, PBTC (20 ppm) + ascorbate (25 ppm); ■, Zn^{2+} (20 ppm) + ascorbate (25 ppm); ●, PBTC (20 ppm) + Zn^{2+} (20 ppm) + ascorbate (25 ppm)

attributed to roughness and inhomogeneities of the solid surface [29]. It is also attributed to the distribution of active sites, adsorption of inhibitor molecules and formation of porous layers [30]. In such cases, the parallel network charge transfer resistance–double layer capacitance ($R_{ct} - C_{dl}$) is a poor approximation especially for systems where an efficient inhibitor is present. Due to the fact that the double layer does not behave as an ideal capacitor in the presence of the dispersing effect, a CPE is substituted for the capacitor to fit the impedance behaviour of the electrical double layer more accurately [31–34]. CPE can thus be regarded as a non-ideal capacitance [35]. The admittance and impedance of a CPE are, respectively, defined as

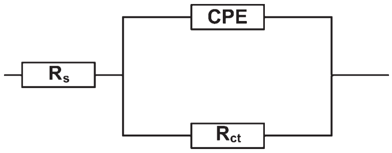

Figure 10. The equivalent circuit used to fit the impedance spectra

$$Y_{CPE} = Y_o\,(j\omega)^n \tag{5}$$

and

$$Z_{CPE} = A\,(j\omega)^{-n} \tag{6}$$

where ω is the angular frequency, Y_o is the modulus which represents different quantities, depending on the value of CPE exponent, n and A is the proportional factor mathematically the reciprocal of modulus [32–34, 36]. For a highly polished electrode, the value of n is close to 1.0. The lower the value of n, the rougher is the electrode surface. It can be seen that when $n = 1$, the element CPE becomes an ideal capacitor. The value of n is also related to the inherent physical and chemical heterogeneous nature of the solid surface, the presence of a porous corrosion product layer and non-uniform distribution of current density on the surface [37–39].

All the Nyquist plots obtained in the present study are characterised by single time constant. The experimental data obtained from these plots are fitted by the equivalent electrical circuit shown in Fig. 10. Such an equivalent circuit was also discussed by several researchers [32, 33, 40], who obtained similar depressed semicircles with single time constant. The impedance parameters, viz. charge transfer resistance (R_{ct}), CPE and CPE exponent (n) obtained from the Nyquist plots and the calculated inhibition efficiency (IE_i) values are shown in Table 3. Charge transfer resistance (R_{ct}) and the non-ideal capacitance (CPE) are the two important parameters related to corrosion processes at the metal/solution interface. The former one is directly related to the rate of corrosion reaction at the interface while the latter is related to the structure of electrical double layer at the interface. During corrosion inhibition by the adsorption of inhibitor molecules,

Table 3. Impedance parameters for carbon steel in 200 ppm NaCl environment in the absence and presence of inhibitor formulations

Concentration (ppm)			Impedance parameters			Inhibition efficiency, IE_i (%)
PBTC	Zn^{2+}	Ascorbate	Charge transfer resistance, R_{ct} ($\Omega\,cm^2$)	Constant phase element, CPE ($\mu F/cm^2$)	n	
0	0	0	2575	13.41	0.592	–
40	0	0	7164	10.13	0.739	64.06
0	40	0	1144	24.07	0.729	−125.09
40	40	0	10 030	7.16	0.618	74.33
20	20	0	4555	10.79	0.676	43.47
20	0	25	5907	9.22	0.654	56.41
0	20	25	6542	11.61	0.598	60.64
20	20	25	16 010	7.95	0.826	83.92

high R_{ct} values can be obtained due to slower corroding system [41, 42]. Consequently, the decrease in CPE can result from the decrease of the local dielectric constant and/or from the increase of thickness of electrical double layer, which suggests an adsorption of the inhibitor molecules on the metal surface [43]. Hence, for an effective inhibition process, there will be an increase in R_{ct} and decrease in CPE. However, there are inhibition processes that are associated with increase in capacitance values. This can be interpreted due to the replacement of water molecules in the interface by ionic inhibitor species and/or due to oxides/hydroxides of metal formed due to initial corrosion. *Bonnel* et al. [44] studied corrosion of carbon steel in neutral chloride solution by impedance technique. They obtained high capacitance values in their studies and ascribed them due to the existence of a layer of the inner corrosion products.

In the present study, in the presence of the control alone, a small semicircle with an R_{ct} value of 2575 Ω is observed. Similar semicircle is also obtained when 40 ppm of Zn^{2+} is added to the control. Due to Zn^{2+} ions, the R_{ct} is decreased and CPE value is increased with a slight increase in the value of n. These changes are due to the replacement of water molecules in the interface by the zinc ions, which resulted in the increased rate of corrosion. By the addition of 40 ppm of PBTC to the control, a single and slightly depressed semicircle with high R_{ct} value is obtained. The capacitance value is decreased and n value is increased. These observations can be attributed to the presence of organic inhibitor molecules in the double layer and the control of corrosion processes to some extent. When the combination of 40 ppm each of PBTC and Zn^{2+} is considered in the presence of control, a large depressed semicircle is observed from high frequency to low frequency regions in the Nyquist plot, indicating that the charge transfer resistance becomes dominant in the corrosion processes due to the presence of protective film on the metal surface. This result is supported by the significant decrease in CPE and a slight increase in n value. In the presence of PBTC/Zn^{2+} combination at 40 ppm each, the capacitive loop is more depressed than that in the presence of 20 ppm each of PBTC and Zn^{2+}. When 25 ppm of ascorbate is added to 20 ppm each of PBTC and Zn^{2+}, a very large capacitive loop with a slight depression is observed. This semicircle represents the R_{ct} value of 16 010 Ω, which is about six times greater than that observed in case of the control. The CPE value at the metal/solution interface is found to decrease from 13.41 μF/cm^2 in case of the control to 7.95 μF/cm^2 in case of the ternary inhibitor formulation. This is because of the replacement of water molecules in the electrical double layer by the organic molecules having low dielectric constants [45]. The value of n is considerably increased to 0.826 in the presence of the ternary inhibitor system suggesting the decrease of inhomogeneity of the interface during inhibition. These results indicate that there is formation of a non-porous and protective film in the presence of the ternary inhibitor formulation. The inhibition efficiency obtained from impedance studies for 1 h immersion period is found to be 83.92%. Several authors, who studied the inhibitory effects of phosphonate-based corrosion inhibitors, also reported that there is formation of thick and less permeable protective film on the metal surface [7, 8, 26]. They also concluded that the protective film consists of phosphonate–metal complexes. The impedance results of the present study also infer the synergistic action operating between PBTC, Zn^{2+} and ascorbate. This is in agreement with the inferences drawn from polarisation and gravimetric studies.

The Nyquist plots for carbon steel in the control and the binary and ternary inhibitor formulations at different immersion periods (1–24 h) and at a constant temperature of 30 °C are shown in Fig. 11. The impedance parameters obtained from these plots and the inhibition efficiencies calculated from R_{ct} values are shown in Table 4. All the Nyquist plots are depressed capacitive loops, which are characterised by single time constant. In case of the control, there is a slight decrease in R_{ct} with immersion period, while CPE is considerably increased to an extent of 9.79 μF/cm^2 after an immersion time of 24 h. The value of n ranges between 0.574 and 0.658. The significant increase in CPE is due to a large increase in the specific area caused by the presence of corrosion products on the metallic surface with time [44]. In case of both the binary and ternary inhibitor formulations, there is an increase of R_{ct} value with increase in immersion time. However, the increase is more in case

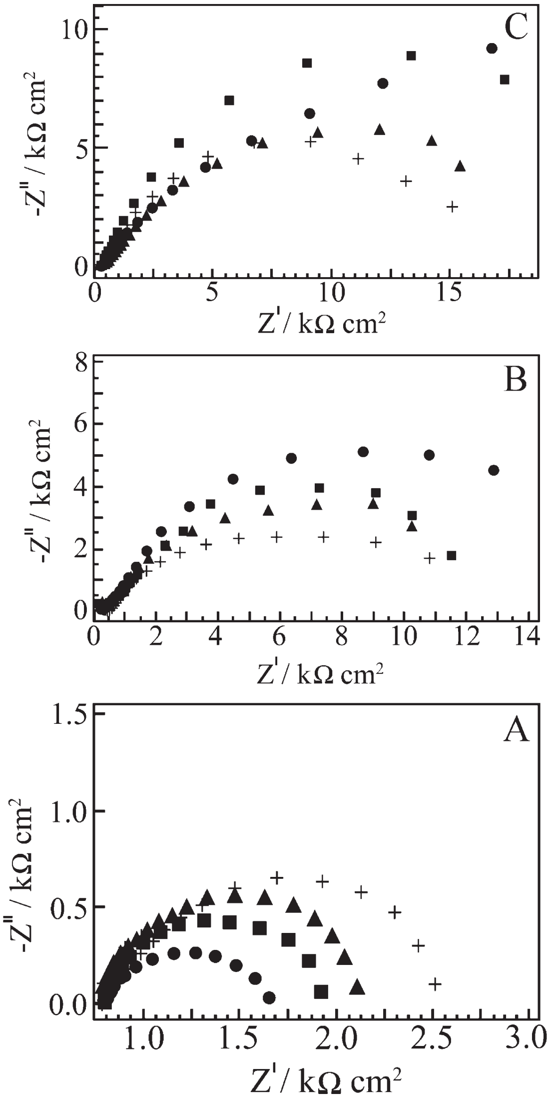

Figure 11. Nyquist plots of carbon steel in the absence and presence of inhibitors at various immersion periods: +, 1 h; ▲, 6 h; ■, 12 h; ●, 24 h. (A) Control, (B) binary inhibitor system, (C) ternary inhibitor system

Table 4. Impedance parameters for carbon steel in 200 ppm NaCl environment in the absence and presence of the binary as well as ternary inhibitor formulations at different immersion periods and at a constant temperature of 30 °C

Immersion time	Impedance parameters			IE (%)
	R_{ct} (Ω cm^2)	CPE (μF/cm^2)	n	
Control – 200 ppm NaCl				
1 h	2575	13.41	0.592	–
6 h	2080	16.85	0.613	–
12 h	1870	18.27	0.574	–
24 h	1598	23.20	0.658	–
Binary inhibitor formulation – PBTC (40 ppm) + Zn^{2+} (40 ppm)				
1 h	10 030	7.16	0.618	74.33
6 h	12 140	6.58	0.648	82.87
12 h	14 210	5.71	0.605	86.84
24 h	20 940	4.72	0.595	92.37
Ternary inhibitor formulation – PBTC (20 ppm) + Zn^{2+} (20 ppm) + ascorbate (25 ppm)				
1 h	16 010	7.95	0.826	83.92
6 h	19 450	6.96	0.855	89.31
12 h	28 370	6.55	0.781	93.41
24 h	45 500	4.36	0.825	96.49

of the ternary inhibitor formulation when compared with the binary formulation at each immersion time studied. CPE is decreased in case of both the formulations almost to the same extent with time. The decrease in CPE may be due to the displacement of hydrated layer at the double layer by the developing inhibitor film on the surface [46]. Supposing that the electrochemical processes are taking place only at the pores and pinholes of the surface film, the increasing R_{ct} values give direct information on the growth and quality of the inhibitor film. Thus, these observations indicate that a continuous build up of inhibitor film is taking place with time resulting in the formation of non-porous and protective layer at the surface. In case of the ternary inhibitor formulation, the values of n at various immersion periods are close to each other, which infer that the homogeneity of the surface film is maintained during the immersion period studied. In case of both the binary and ternary inhibitor formulations, depressed nature is more for the semicircles obtained at an immersion time of 24 h. The inhibitor film formed after an immersion period of 24 h by all the three components of the ternary inhibitor formulation resulted in the rapid fall of the rate of iron dissolution of the substrate, as indicated by its highest inhibition efficiency of 96.49%. From these studies, it may be noted that this highest inhibition efficiency, achieved after an immersion time of 24 h, is close to that obtained by gravimetric measurements. It is inferred that an immersion time of 24 h is required for the formation of the protective film.

Figure 12 presents the Nyquist plots for carbon steel in the control and the binary and ternary inhibitor formulations at different temperatures. The impedance parameters obtained from these plots and the inhibition efficiencies calculated from R_{ct} values are shown in Table 5. All the Nyquist plots are depressed capacitive loops, which are characterised by single time constant. In case of the control, there is a slight decrease in R_{ct} and an increase in CPE with temperature. The value of n is decreased from 0.658 at 30 °C to 0.149 at 60 °C. It is obvious that these changes are due to enhanced corrosion reactions at both the anodic and cathodic sites with increasing temperature in the absence of any inhibitor. It can be observed that in case of both the binary and ternary inhibitor formulations, the size of the

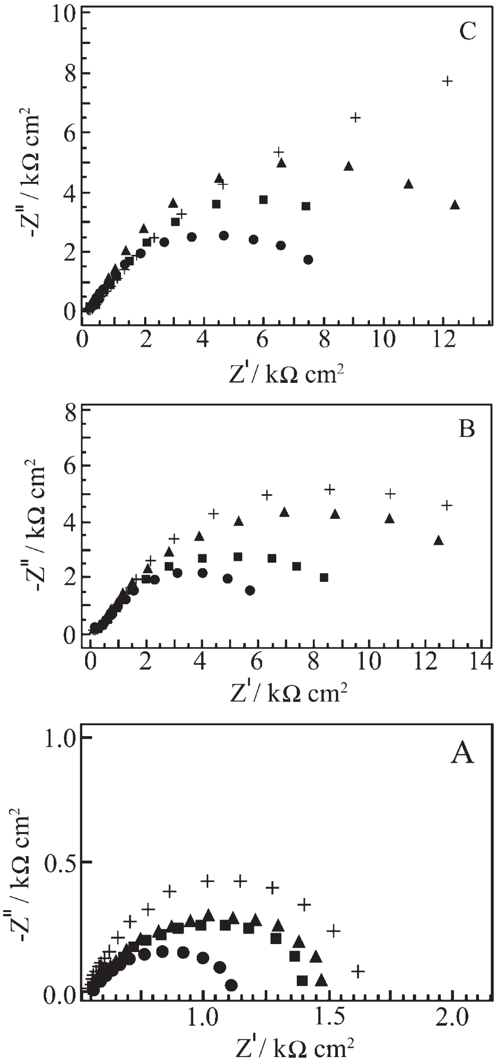

Figure 12. Nyquist plots of carbon steel in the absence and presence of inhibitors at various temperatures: +, 30 °C; ▲, 40 °C; ■, 50 °C; ●, 60 °C. (A) Control, (B) binary inhibitor system, (C) ternary inhibitor system

Table 5. Impedance parameters for carbon steel in 200 ppm NaCl environment in the absence and presence of the binary as well as ternary inhibitor formulations at different temperatures and constant immersion period of 1 h

Temperature (°C)	Impedance parameters			IE (%)
	R_{ct} (Ω cm^2)	CPE (μF/cm^2)	n	
Control – 200 ppm NaCl				
30	1598	23.20	0.658	–
40	1494	25.90	0.440	–
50	1446	29.40	0.262	–
60	1198	30.90	0.149	–
Binary inhibitor formulation – PBTC (40 ppm) + Zn^{2+} (40 ppm)				
30	20 940	4.72	0.595	92.37
40	15 580	7.21	0.647	90.41
50	12 020	7.38	0.574	87.97
60	8636	7.77	0.523	86.13
Ternary inhibitor formulation – PBTC (20 ppm) + Zn^{2+} (20 ppm) + ascorbate (25 ppm)				
30	45 500	4.36	0.825	96.49
40	17 270	5.96	0.740	91.35
50	14 800	8.23	0.734	90.23
60	11 590	9.52	0.419	89.66

capacitive loop is gradually decreased with increase of temperature. In the presence of the binary system, the R_{ct} value is gradually decreased with temperature, while in case of the ternary system, a rapid fall of R_{ct} is observed from the temperature 30 to 40 °C and later the fall is gradual. From the results given in Table 5, it is clear that at each temperature in the studied region, the inhibition efficiencies are slightly higher for the ternary inhibitor system than that for binary formulation. In case of the binary inhibitor formulation, CPE is increased with temperature from 30 to 40 °C and later it is almost constant at further elevated temperatures. There is no much influence of temperature on the value of n. But in the presence of the ternary inhibitor formulation, there is increase of CPE with temperature and the value of n decreased from 0.825 to 0.419. These observations can be attributed to the slight dissolution at the local areas of the protective film already present on the surface, making it slightly porous and inhomogeneous. It may also be due to desorption of some of the adsorbed inhibitor species at relatively higher temperatures. However, the inhibition efficiency is nearly 90% even at 60 °C. Hence, it can be concluded that this ternary inhibitor system is efficient in the corrosion control of carbon steel at elevated temperatures even up to 60 °C.

A significant observation related to the inhibition efficiency values is to be noted. If the inhibition efficiencies obtained from gravimetric (IE_w), polarisation (IE_p) and EIS (IE_i) studies are compared, slight differences are observed. The IE values obtained from R_{ct} are closer to those obtained from the gravimetric measurements, when compared with the values obtained from polarisation data. It is suggested that the inhibition efficiency values obtained from various methods may not be strictly compared as the immersion times considered for all these methods are not same.

3.4 X-ray photoelectron spectroscopic studies (XPS)

The XPS deconvolution spectra of the individual elements present in the surface films in the absence and presence of inhibitors are shown in Figs. 13–17. The interpretation of all these spectra is done with the help of the data of the elemental binding energies reported in the literature and also with the help of the reports published on the analysis of XPS spectra of the surface films.

The Fe 2p deconvolution spectrum in case of the control is shown in Fig. 13A. Two peaks are observed, one at 710.8 eV

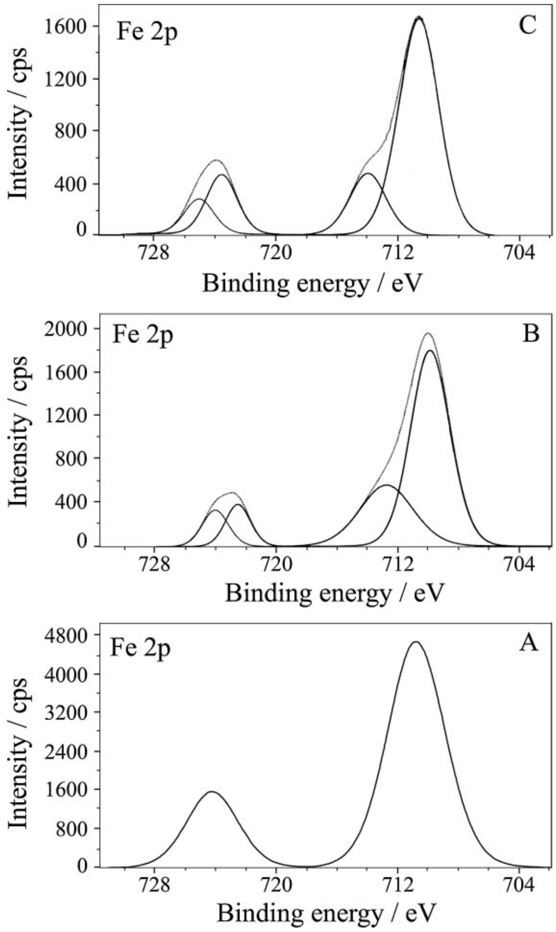

Figure 13. XPS deconvolution spectra of Fe 2p in the surface films. (A) Control, (B) binary inhibitor system, (C) ternary inhibitor system

corresponding to Fe $2p_{3/2}$ and the other one at 724.2 eV corresponding to Fe $2p_{1/2}$ electron. The peak due to Fe $2p_{3/2}$ is interpreted for the determination of chemical state of iron in the surface film. The peak of Fe $2p_{3/2}$ at 710.8 eV is the one, shifted from 707.0 eV, the characteristic elemental binding energy of Fe $2p_{3/2}$ electron [47]. Such a large shift of 3.8 eV suggests that iron is present in Fe^{3+} state in the surface film. In the literature [26, 48], the peak at 711.0 eV was ascribed to the presence of FeOOH and $Fe(OH)_3$. The binding energy of Fe $2p_{3/2}$ due to γ-Fe_2O_3 was reported to be 711.0 ± 0.15 eV [49]. It was also reported that the mean binding energy of Fe $2p_{3/2}$ in α-FeOOH is 711.0 ± 0.2 eV [49]. *Maroie* et al. [50] reported that the binding energy value of 711.0 eV for Fe $2p_{3/2}$ is due to ferric oxide species. Thus, the presence of a peak due to Fe $2p_{3/2}$ observed in case of the control at 710.8 eV can be ascribed due to the presence of iron in the form of γ-Fe_2O_3, Fe_3O_4 and FeOOH. The spectrum (Fig. 13B) corresponding to the binary inhibitor system shows the Fe $2p_{3/2}$ peak at 710.4 eV and also a peak at 713.1 eV. Similarly in the case of the ternary inhibitor system also, the XPS (Fig. 13C) shows the Fe $2p_{3/2}$ peak at 710.8 eV and the other peak at 714.2 eV. Thus, the Fe $2p_{3/2}$ peaks obtained in the case of both the binary and ternary formulations infer the presence of oxides and hydroxides like Fe_2O_3, Fe_3O_4, FeOOH and also involvement of Fe^{3+} in the complex formation with the inhibitor molecules. No peak is observed due to elemental iron in the case of control and also in the case of both binary and ternary inhibitor formulations. This result infers the formation of thick films in all the three cases. The film is porous and non-protective in the case of control and non-porous and highly protective in the presence of inhibitor molecules. If the intensities of Fe $2p_{3/2}$ peaks are compared, they are 4600 cps for control, only 1800 cps for binary inhibitor system and 1700 cps for ternary inhibitor system. Such a large decrease in the intensity of Fe 2p peak in the presence of both the inhibitor formulations can be understood because of formation of protective films and consequently less corrosion of iron and less amount of iron oxide. The binding energy of Fe^{2+} state in iron oxides is reported to be around 708.5 eV [51]. The absence of any peak in this region in the present study also supports that iron does not exist in Fe^{2+} state.

The XPS spectra of phosphorus are shown in Fig. 14. In case of the binary formulation, the P 2p peak is observed at 133.0 eV, while in case of the ternary formulation, it is observed at 133.1 eV. In the literature [52, 53], it was reported that the P 2p peak could be observed in the range of 132.9–133.8 eV, for iron or steels immersed in the solutions containing phosphonates, orthophosphates and polyphosphates. *Nakayama* [54] obtained a P 2p peak at 133.0 eV and attributed it to the presence of phosphonate compounds. *Felhosi* [7] et al. observed a P 2p peak at 132.1 eV in the XPS of the surface film formed on carbon steel when immersed in a solution containing Zn^{2+} and HEDP. They interpreted this peak due to the presence of [Zn–HEDP] complex in the surface film. *Ochoa* et al. [55] in their studies on the mixtures of salts of phosphonocarboxylic acids and fatty amines as inhibitors for corrosion of carbon steel reported the P 2p peak at 132.1 eV and interpreted it due to the presence of phosphonate group in the surface film. In the light of these reports, the P 2p peaks observed in the present study suggest the presence of PBTC in the surface films formed in the case of both binary and ternary inhibitors. The intensity of the P 2p peak in case of the ternary inhibitor formulation is found to be one fourth of the intensity of P 2p peak in case of the binary formulation while the concentration of PBTC is reduced to only half in the ternary inhibitor formulation in comparison to the binary system. This infers the presence of ascorbate also in the protective film, as evidenced by a high intensity C 1s spectrum in the case of ternary formulation.

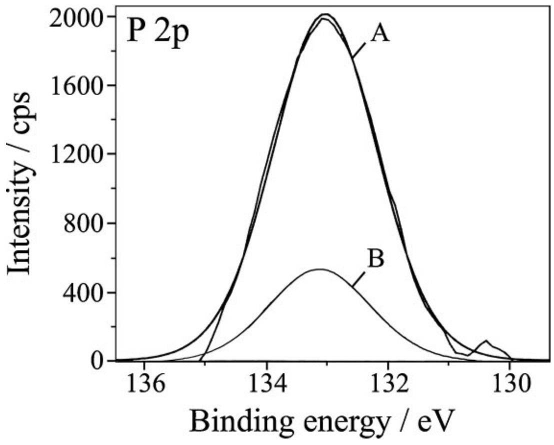

Figure 14. XPS deconvolution spectra of P 2p in the surface films. (A) Binary inhibitor system, (B) ternary inhibitor system

The XPS spectra of C 1s are shown in Fig. 15. C 1s spectrum in case of the control shows a single peak at 284.6 eV. This peak is due to contamination from the vacuum system and chamber during the analysis [56]. In case of the binary formulation, the C 1s spectrum (Fig. 15B) has two peaks, one is the high intense peak at 284.5 eV and the other one is a low intense peak at 288.3 eV. *Ochoa* et al. [55] in their studies on the mixtures of salts of phosphonocarboxylic acids and fatty amines as inhibitors for corrosion of carbon steel reported the C 1s peak at 284.5 eV. This signal was accounted for by the presence of the inhibitor molecules on the steel surface. *Gunasekaran* and *Chauhan* [32] studied the corrosion inhibition of mild steel by a plant extract and they obtained C 1s peaks at 285, 287 and 288.6 eV. They interpreted these peaks due to C–C, C–O and C=O bonds because of the organic molecules present in the plant extract. *Aramaki* and *Shimura* [57] obtained a peak of organic carbon at 284.5 eV and they inferred that it is due to adsorbed organic inhibitor molecules on the surface. PBTC has various carbon environments and hence the two peaks observed in the presence of the binary formulation indicate the presence of PBTC in the surface film. In case of the ternary inhibitor formulation, a relatively more intense peak was observed at 284.6 eV along with a small peak at 288.4 eV. The increase in intensities of the peaks in the presence of ternary inhibitor system indicates that both PBTC and ascorbate ions are present in the surface film.

The XPS spectra of O 1s are presented in Fig. 16. In case of the control (Fig. 16A), two peaks corresponding to O 1s are observed, one at 530.1 eV and the other one at 533.0 eV. The latter peak is essentially due to adsorbed water on the surface. Several researchers have obtained O 1s peak around 533.0 eV and ascribed it due to water molecules adsorbed on the metal surface [51, 54, 58]. *Ochoa* et al. [55] obtained O 1s peak at 533.2 eV and attributed it to the presence of water molecules adsorbed on the oxide/hydroxide mixture. In the present study, O 1s peak

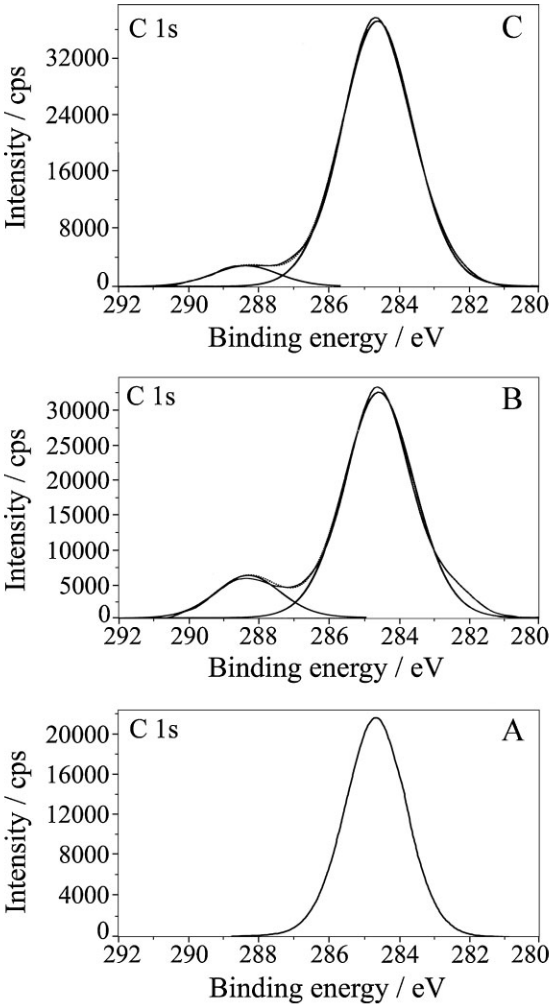

Figure 15. XPS deconvolution spectra of C 1s in the surface films. (A) Control, (B) binary inhibitor system, (C) ternary inhibitor system

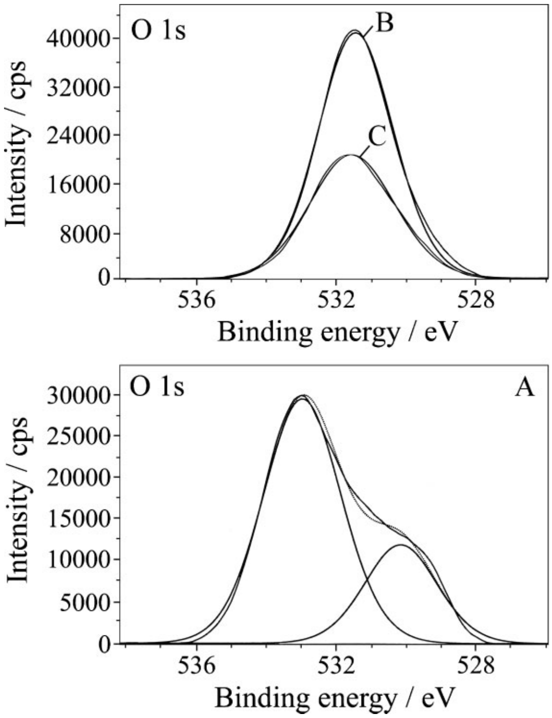

Figure 16. XPS deconvolution spectra of O 1s in the surface films. (A) Control, (B) binary inhibitor system, (C) ternary inhibitor system

observed at 530.1 eV is due to O^{2-}. *Pech-Canul* and *Bartolo-Perez* [26] obtained O 1s peak at approximately 529.8 eV and attributed it to O^{2-}. *Karman* et al. [58] studied the role of oxide layer formation during corrosion inhibition of mild steel in neutral aqueous media. They assigned the O 1s peak at ~530 eV to O^{2-}. In the present study, the presence of O^{2-} in the surface film formed in the presence of control may be in the form of oxides/hydroxides of Fe(III). In case of both the binary and ternary inhibitor formulations, a single O 1s peak of high intensity was observed. It is positioned at 531.4 eV in the former case and at 531.5 eV in the latter case. *Fang* et al. [59] ascribed the O 1s peak observed at 531.3 eV to the complex formed between iron and phosphonate. *Pech-Canul* and *Bartolo-Perez* [26] observed the O 1s peak at 531.3 eV, which was ascribed to OH^- from hydrous iron oxides and to the complex formed between iron and phosphonate group. It was also mentioned in their article that such hydrous ferric oxides consist of $Fe(OH)_3$ and FeOOH. *Felhosi* et al. [7] studied effects of bivalent cations on corrosion inhibition of steel by HEDP. They mentioned that the O 1s peak at 531.4 eV is due to Fe–OH bond. *Asami* et al. [51] observed O 1s peak at 531.5 eV in their study and attributed it to oxygen with a kind of Fe–O–H bond. In the light of these results and interpretations reported in the literature, the O 1s peaks of high intensity observed in the present study may be interpreted as follows. The XPS of surface films show that besides oxygen, there is presence of carbon, phosphorus, iron and zinc in the surface films. That means PBTC is present on the surface, zinc is present as Zn^{2+} and the interpretation given above in case of Fe 2p indicates the presence of Fe_2O_3, Fe_3O_4 and FeOOH. Hence, O 1s peaks can be ascribed to the presence of $Zn(OH)_2$, Fe_2O_3, Fe_3O_4, FeOOH and oxygen of PBTC in the surface film. In case of the ternary inhibitor formulation, O 1s peak can also be ascribed to –OH group of ascorbate ion in addition to the presence of all the compounds mentioned above in the case of binary inhibitor formulation. The disappearance of the peak around 533 eV in case of the binary and ternary inhibitor formulations indicates the absence of water molecules in the surface films as they have been completely replaced by the inhibitor molecules.

A comparison of intensities of O 1s peak in the control, in the presence of binary inhibitor system and in the presence of ternary inhibitor system is of interest. In comparison to the intensity of 29 500 cps in control, the intensity of O 1s peak increases to 40 000 cps in the presence of binary inhibitor system. This increase is to be considered along with the large intensity of zinc (Fig. 17A), of carbon (Fig. 15B) and of phosphorus (Fig. 14). The intensity of O 1s peak is related mainly to oxygen in one phosphonate and three carboxylate groups of PBTC, –OH group of $Zn(OH)_2$ and to small amounts of oxides/hydroxides of iron. Interestingly, the intensity of O 1s peak in the case of ternary inhibitor system is reduced to 20 500 cps, which is almost equal to half of the intensity of O 1s peak in the case of binary inhibitor system. This is because of the reduction in the concentrations of

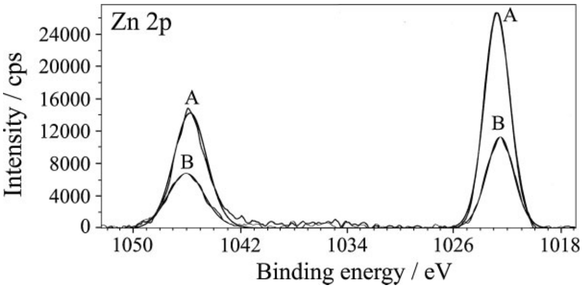

Figure 17. XPS deconvolution spectra of Zn 2p in the surface films. (A) Binary inhibitor system, (B) ternary inhibitor system

PBTC and Zn^{2+} to half in the ternary system, though there is an addition of 25 ppm of ascorbate, equivalent to 1.42×10^{-4} M. This can be seen in combination with reduction in the intensities of Zn 2p and P 2p peaks in the spectrum of the ternary system.

Figure 17 presents the XPS deconvolution spectra of zinc. In case of the binary formulation, the Zn $2p_{3/2}$ peak is observed at 1022.8 eV and the Zn $2p_{1/2}$ peak at 1045.7 eV. In case of the ternary formulation, these peaks are observed at 1022.7 and 1045.8 eV, respectively. Zn $2p_{3/2}$ peak is normally interpreted. The high intensities of the Zn $2p_{3/2}$ peaks observed in both the spectra may be ascribed to the presence of $Zn(OH)_2$ in the surface film and also to the involvement of Zn^{2+} in the complex formation with PBTC. In case of the ternary formulation, zinc ions involve in the complex formation with both PBTC and ascorbate ions. It was reported in the literature by *Aramaki* [60] that the Zn $2p_{3/2}$ peak at 1022.7 eV was due to the presence of $Zn(OH)_2$ in the surface film. *Felhosi* et al. [7] interpreted from the XPS analysis that there is formation of [Zn–HEDP] complex on the mild steel surface when immersed in a solution consisting of a mixture of HEDP and Zn^{2+}. In the present study, the intensity of Zn 2p peak in case of the ternary formulation is less than half of the intensity of the corresponding Zn 2p peak obtained in the case of the binary inhibitor formulation. This is because the bulk concentration of Zn^{2+} in case of the ternary system is half of that of the binary system.

Along with the elements discussed above, the survey spectrum (not shown) in case of the control has a low intensity chlorine peak at 200.0 eV. This is because some chloride ions reach the metal surface and are responsible for corrosion of the metal. The chlorine peak is not observed in the survey spectra of inhibited surface films, which indicates that the protective films are non-porous and do not allow the aggressive ions to reach the metal surface. After consolidating all the inferences drawn from the XPS of individual elements present in surface films, it is suggested that the surface film consists of mainly [Zn(II)–PBTC] complex, $Zn(OH)_2$ and small amounts of oxides/hydroxides of Fe(III) in the case of binary inhibitor system. In the case of ternary inhibitor system, the surface film may consist of ternary complex namely [Zn(II)–PBTC–ascorbate], $Zn(OH)_2$ along with Fe(III) oxides/hydroxides. The complex may be chemisorbed on the metal surface and get attached to the Fe(III) ions.

3.5 Interpretation of FTIR spectra

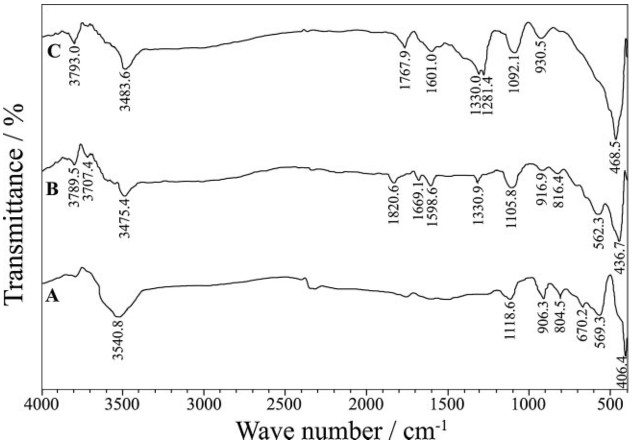

Figure 18. Reflection absorption FTIR spectra of the surface films. (A) Control, (B) binary inhibitor system, (C) ternary inhibitor system

The reflection absorption FTIR spectra of the surface films formed on carbon steel in the absence and presence of the binary and ternary inhibitor formulations are shown in Fig. 18. These spectra are interpreted by comparing with the FTIR spectra of pure PBTC and pure ascorbic acid (not shown here) as well as with the help of literature reports. In the FTIR spectrum of PBTC, multiple bands in the region, 900–1150 cm^{-1} were assigned to $–PO_3$ stretching frequencies [61]. The peak at 1200 cm^{-1} was assigned to P=O group while the peak at 926 cm^{-1} was assigned to P–OH group [62, 63]. In case of the inhibited surface film formed by the binary formulation in the present study, the peak due to P=O is shifted from 1200 to 1105.8 cm^{-1}, while in case of the ternary formulation, it is shifted to 1092.1 cm^{-1}. The P–OH stretching located at 916.9 cm^{-1} in case of the binary formulation and at 930.5 cm^{-1} in case of the ternary formulation is observed to be weak. These results can be interpreted in terms of interaction between $P–O^-$ present in the phosphonate with metallic species, viz. Zn(II) and Fe(III) to form P–O–Zn and P–O–Fe bonds. This interpretation was also given by several authors, who worked on corrosion inhibition of carbon steel by phosphonates [8, 23, 64]. *Carter* et al. [65] found that FTIR spectra obtained with an organic phosphonate on a steel substrate are consistent with the phosphonate reaction on steel to produce a metal salt. This also suggests that phosphonates are coordinated with metal ions resulting in the formation of [metal–phosphonate] complexes on the metal surface. Weak bands observed in both the spectra (Fig. 18B,C) around 1330 cm^{-1} indicate the presence of zinc hydroxide in the surface film [2, 4, 64]. A very broad and intense band around 1716 cm^{-1} in the FTIR spectrum of PBTC was reported [66]. This is characteristic of uncoordinated, protonated carboxylate and was assigned to the C=O stretch of –COOH. In the FTIR spectrum of pure ascorbic acid, the C=O stretching frequency is observed at 1669.1 cm^{-1}. In case of the binary inhibitor formulation of the present study, the C=O stretching frequency is observed by a strong absorption band at 1676 cm^{-1}. The small peaks at 1767.9 and 1601.0 cm^{-1} in the reflection absorption FTIR spectrum of the surface film in case of the ternary inhibitor system indicate the presence of both PBTC and ascorbate ions in the surface film. The shifts in the stretching frequency are resulted due to the involvement of these ions in the complex formation. There are several bands in the region, 1200–400 cm^{-1} in all the spectra of surface films. Many of these peaks imply the presence of various oxides and hydroxides of iron like Fe_3O_4, FeOOH and Fe_2O_3 [54, 57]. *Yee* and *Chow* [67] obtained peaks at 570 and 630 cm^{-1} and assigned them to amorphous oxides of Fe_2O_3 and Fe_3O_4. *Amar* et al. [64] obtained absorption peaks between 750 and 1100 cm^{-1}, in the spectra of metal surfaces in the presence of 3% NaCl solution. They interpreted them to corrosion products of ferric hydroxide (γ-FeOOH) and magnetite (Fe_3O_4). A moderately intense and a broad band formed at 3540.8 cm^{-1}, in case of the control, can be assigned to the presence of –OH group on the surface. This hydroxyl group may be in the form of FeOOH and/or $Fe(OH)_3$ [68]. Such peaks are observed in the spectra of the inhibited surface films also. These peaks can be assigned to the –OH groups present in the inhibitor molecules, to $Zn(OH)_2$ and a small contribution of hydroxide of Fe(III) present in the inhibited films.

Thus, the reflection absorption FTIR spectrum of the surface film formed in the presence of the binary inhibitor formulation infers the presence of [Zn(II)–PBTC] complex, $Zn(OH)_2$ and small amounts of oxides and hydroxides of Fe(III). In case of the ternary inhibitor system, the complex formed is [Zn(II)–PBTC–ascorbate].

The XPS spectra and the reflection absorption FTIR spectra of the surface films infer the presence of Fe(III), Zn(II), PBTC and ascorbate in the surface films. The shifts in binding energies of various elements and shifts in the absorption band frequencies of various functional groups inferred that PBTC and ascorbate are involved in the complex formation with Zn^{2+} and Fe^{3+}. This inference is further supported by several studies reported in literature. *Holm* et al. [69] studied the nature of the film formed on carbon steel in cooling water in the presence of an inhibitor containing 20 ppm of PBTC and 200 ppm of Ca^{2+} ions by XPS and AES techniques. They interpreted that PBTC is present as deprotonated Ca(II)–PBTC complex, which reacts with the Fe(III) ions at the steel surface to form cross-linked, amorphous, anhydrous Fe(III)–Ca(II)–PBTC compound. *Mao* and *Clearfield* [70] synthesised a ternary zinc complex with a phosphonic acid namely *N*-(phosphonomethyl)iminodiacetic acid (PMIDA) and a carboxylic acid namely acetic acid. They reported that the crystal structure of that complex, $Zn_2(PMIDA)(CH_3COOH)\cdot 2H_2O$, features a two-dimensional zinc carboxylate–phosphonate hybrid layer. *Kuznetsov* [71] reported that the mechanism of action of phosphonates is not only associated with adsorption but also with electrophillic substitution of complex-forming surface cations, precipitation of almost insoluble hydroxides and formation of hetero- and polynuclear complexes. *Freedman* [72] reported in his study on cooling water systems that though the key role of zinc ions in corrosion inhibition is to precipitate zinc hydroxide on the metal surface, in some cases, the zinc ions also complex with the stabilising agents. *Shaban* et al. [73] studied the inhibitive effect of *N*-phosphonomethyl glycine (NPMG) on corrosion of steel. One of their interpretations was that Ca^{2+} and Zn^{2+} ions form a passivating complex with NPMG on the steel surface, which protects the metal. *Felhosi* et al. [7] studied the effects of bivalent cations on corrosion inhibition of steel by HEDP. They interpreted their XPS results in terms of formation of complex between HEDP and Zn^{2+} on the carbon steel surface. They mentioned that there is formation of heteropolynuclear complexes on the iron surface. *Gonzalez* et al. [8] studied the synergistic effect between amino-trimethyl phosphonic acid (ATMP) and zinc chloride in corrosion inhibition of carbon steel with 0.5 M NaCl as the control. They reported that ATMP forms chelate compounds with Zn^{2+} and Fe^{3+} and it leads to the enhancement of the corrosion protection due to construction of a dense system, which prevents the penetration of aggressive species. Based on all these literature reports on various phosphonates and the requirement of optimum concentration of zinc ions for effective inhibition and also on the high intensity Zn 2p peaks obtained from XPS spectra, it can be inferred that Zn(II) and Fe(III) are involved in the complex formation with PBTC and ascorbate to form [Fe(III), Zn(II)–PBTC–ascorbate] polynuclear multiligand complex, which plays significant role in making the surface film protective.

3.6 Mechanism of corrosion protection

In order to explain all the experimental results, a plausible mechanism of corrosion inhibition is proposed as follows:

1. The mechanism of corrosion of carbon steel in nearly neutral aqueous media is well established. The well-known reactions are mentioned below

   $$Fe \rightarrow Fe^{2+} + 2e^- \tag{7}$$

   Fe^{2+} further undergoes oxidation in the presence of oxygen available in the aqueous solution

   $$Fe^{2+} \xrightarrow{[O_2]} Fe^{3+} + e^- \tag{8}$$

   The corresponding reduction reaction at cathodic sites in neutral and alkaline media is

   $$O_2 + 2H_2O + 4e^- \rightarrow 4OH^- \tag{9}$$

   Fe^{3+} ions produced at anodic areas and OH^- ions produced at cathodic areas combine to form $Fe(OH)_3$, ($Fe_2O_3\cdot H_2O$) which gets precipitated on the surface of the metal due to its very low solubility product (K_{sp} of $Fe(OH)_3 = 1.1 \times 10^{-36}$).
2. When PBTC and Zn^{2+} ions are added to the aqueous solution, PBTC reacts with Zn^{2+} to form a binary complex, [Zn^{2+}–PBTC]. It diffuses to the metal surface and binds to Fe(III) ions present on the surface. The cross-linkage and reorganisation of such complex ions on the surface will produce a polymeric network structure. The resulting polynuclear complex, [Fe(III), Zn(II)–PBTC] covers the anodic sites and controls the corresponding anodic reaction

   $$[Zn(II) - PBTC] + Fe^{3+} \rightarrow [Fe(III),\ Zn(II) - PBTC] \tag{10}$$

3. In case of the ternary inhibitor formulation, both PBTC and ascorbate react with Zn^{2+} to form a ternary complex, [Zn^{2+}–

PBTC–ascorbate]. This complex diffuses to the metal surface and binds with Fe(III) ions available on the metal surface. A dense polymeric network structure is constituted on the surface by high degree of cross-linkage and reorganisation. The polynuclear multiligand complex [Fe(III), Zn(II)–PBTC–ascorbate] covers the anodic sites and controls the anodic reaction of the corrosion process. *Felhosi* et al. [74] showed that iron can be passivated by simple immersion of it in aqueous solutions of 1,7-diphosphonoheptane. The formation of protective layer by the phosphonate consists of a fast adsorption step and subsequent slower process, which is supposed to be due to the organisation. According to the authors, this effect is due to the formation of self-assembling layer of complexes of the organic inhibitor with iron

$$[\mathrm{Zn(II)-PBTC-ascorbate}] + \mathrm{Fe}^{3+} \rightarrow [\mathrm{Fe(III),\ Zn(II)-PBTC-ascorbate}] \qquad (11)$$

4. Free Zn^{2+} ions are available in the bulk of the solution because of relatively higher molar concentration of Zn^{2+} in the inhibitor mixture. These Zn^{2+} ions diffuse to the metal surface and react with OH^- ions produced at the cathodic sites to form a precipitate of $Zn(OH)_2$

$$\mathrm{Zn}^{2+} + 2\mathrm{OH}^- \rightarrow \mathrm{Zn(OH)}_2 \qquad (12)$$

The precipitate of $Zn(OH)_2$ ($K_{sp} = 1.8 \times 10^{-14}$) gets deposited on the cathodic sites and controls the cathodic partial reaction of corrosion process.
5. The decrease in inhibition efficiency when the bulk concentration of ascorbate is higher than the optimum value can be explained as follows. It may be noted that the molar ratios of Zn^{2+}/PBTC/ascorbate in the bulk of the solution are 4.2:1:8 and 4.2:1:12, when the inhibition efficiencies are found to be very less. When the bulk concentration of ascorbate is so much higher in comparison to that of PBTC (8- to 12-fold higher), the nature and composition of the complex [Zn(II)–PBTC–ascorbate] may be entirely different, with more ascorbate than PBTC. Such a complex may not be protective. Secondly, more free ascorbate is available in the bulk of the solution. This free ascorbate diffuses to the steel surface and gets chemisorbed on the metal surface. To that extent, the protective [Zn(II)–PBTC–ascorbate] complex will not be available on the metal surface. It must be noted that ascorbate alone does not afford significant inhibition [11].
6. The ternary inhibitor formulation is effective in the pH range, 5–8. At pH 9, higher concentration of OH^- ions are available both in the bulk of the solution and on the surface. In such an environment, there is greater interference of OH^- ions in the complexation [21] leading to the formation of [Zn(II)–PBTC–ascorbate–OH] complex, which may not contribute to the formation of protective film on the metal surface. In acidic medium at pH 4, the ligands will be in the protonated form and do not coordinate with Zn(II) as effectively as the deprotonated ligands. Secondly, enough amount of $Zn(OH)_2$ will not be formed on the cathodic sites. Hence, the observed decrease in inhibition efficiency at pH 4.
7. Thus, PBTC, Zn^{2+} and ascorbate play a very important role in the synergistic effect in controlling corrosion through the formation of protective film on the metal surface. It is inferred that the film may consist of various oxides/hydroxides like Fe_2O_3, $Fe_3O_4{\cdot}H_2O$, FeOOH, $Zn(OH)_2$ and a polynuclear multiligand complex, [Fe(III), Zn(II)–PBTC–ascorbate]. Each of these constituents contributes itself to make the film highly protective.

4 Conclusions

1. Both the binary inhibitor system, PBTC–Zn^{2+} and the ternary inhibitor system, PBTC–Zn^{2+}–ascorbate, exhibit excellent synergism in the corrosion control of carbon steel in nearly neutral aqueous environment. The synergistic effect of ascorbate is established.
2. The ternary formulation containing 20 ppm each of PBTC and Zn^{2+} along with 25 ppm of ascorbate is as effective as the binary formulation containing 40 ppm each of PBTC and Zn^{2+}. Once the protective film is formed, a mixture of only 10 ppm each of PBTC and Zn^{2+} and 15 ppm of ascorbate will serve as the maintenance dosage. The ternary inhibitor system is relatively more environmentally friendly.
3. The ternary inhibitor system is effective in the pH range of 5–8.
4. The ternary inhibitor formulation acts as mixed type inhibitor controlling both the anodic and cathodic reactions.
5. Electrochemical impedance studies indicated the significant modification of the metal/solution interface by the formation of dense, non-porous and protective film in the presence of the ternary inhibitor formulation.
6. The formation of protective film on the metal surface requires 24 h immersion time.
7. The ternary inhibitor formulation affords good inhibition efficiency even at a higher temperature of 60 °C.
8. The protective film consists of mainly [Zn(II)–PBTC–ascorbate] complex, $Zn(OH)_2$ and small amounts of oxides/hydroxides of Fe(III). The presence of optimum amounts of all these compounds is required at a given pH value to make the surface film protective.

5 References

[1] J. Telegdi, M. M. Shaglouf, A. Shaban, F. H. Karman, I. Betroti, M. Mohai, E. Kalman, *Electrochim. Acta* **2001**, *46*, 3791.
[2] G. Gunasekaran, N. Palaniswamy, B. V. Appa Rao, V. S. Muralidharan, *Electrochim. Acta* **1997**, *42*, 1427.
[3] L. Y. Reznik, L. Sathler, M. J. B. Cardoso, M. G. Albuquerque, *Mater. Corros.* **2008**, *59*, 685.
[4] I. Sekine, Y. Hirakawa, *Corrosion* **1986**, *42*, 272.
[5] H. S. Awad, *Corros. Eng. Sci. Technol.* **2005**, *40*, 57.

[6] Y. Gonzalez, M. C. Lafont, N. Pebere, G. Chatainier, J. Roy, T. Bouissou, *Corros. Sci.* **1995**, *37*, 1823.

[7] I. Felhosi, Zs. Keresztes, F. H. Karman, M. Mohai, I. Bertoti, E. Kalman, *J. Electrochem. Soc.* **1999**, *146*, 961.

[8] Y. Gonzalez, M. C. Lafont, N. Pebere, F. Moran, *J. Appl. Electrochem.* **1996**, *26*, 1259.

[9] E. Kalman, Presented at *7th European Symposium on Corrosion Inhibitors (7SEIC)*, Ann. Univ. Ferrara, N.S., Sez. V, **1990**, p. 745.

[10] G. Gunasekaran, R. Natarajan, N. Palaniswamy, *Corros. Sci.* **2001**, *43*, 1615.

[11] B. V. Appa Rao, S. Srinivasa Rao, M. Venkateswara Rao, *Corros. Eng. Sci. Technol.* **2008**, *43*, 46.

[12] G. Gunasekaran, R. Natarajan, B. V. Appa Rao, N. Palaniswamy, V. S. Muralidharan, *Indian J. Chem. Technol.* **1998**, *5*, 91.

[13] RPA Report J480b, *Non-surfactant organic ingredients and zeolite-based detergents*, Scientific Committee on Health and Environmental Risks – European Commission, **2006**.

[14] R. Ashcraft, G. Bohnsack, R. Holm, R. Kleinstueck, S. Storp, *Mater. Perform.* **1988**, *27*, 332.

[15] G. Bohnsack, K. H. Lee, D. A. Johnson, E. Buss, *Mater. Perform.* **1986**, *25*, 32.

[16] J. Cape, D. Cook, D. Williams, *J. Chem. Soc., Dalton Trans.* **1974**, 1849.

[17] J. Maslowska, A. Owczarek, *Pol. J. Chem.* **1981**, *55*, 271.

[18] ASTM Standard G 31-72, *'Standard Practice for Laboratory Immersion Corrosion Testing of Materials' (Reapproved 1990), Annual Book of ASTM Standards 0302,* ASTM, Philadelphia, PA, **1990**.

[19] R. A. Freeman, D. C. Silverman, *Corrosion* **1992**, *48*, 463.

[20] M. Elachouri, M. S. Hajju, M. Salem, S. Kertit, J. Aride, R. Coudert, E. Essassi, *Corrosion* **1996**, *52*, 103.

[21] V. Deluchat, J.-C. Bollinger, B. Serpaud, C. Caullet, *Talanta* **1997**, *44*, 897.

[22] B. Zumreoglu-Karan, *Coord. Chem. Rev.* **2006**, *250*, 2295.

[23] X. H. To, N. Pebere, N. Pelaprat, B. Boutevin, Y. Hervaud, *Corros. Sci.* **1997**, *39*, 1925.

[24] S. Rajendran, B. V. Appa Rao, N. Palaniswamy, *Bull. Electrochem.* **2001**, *17*, 171.

[25] E. S. Ferreira, C. Giacomelli, F. C. Giacomelli, A. Spinelli, *Mat. Chem. Phys.* **2004**, *83*, 129.

[26] M. A. Pech-Canul, P. Bartolo-Perez, *Surf. Coat. Technol.* **2004**, *184*, 133.

[27] S. Rajendran, B. V. Appa Rao, N. Palaniswamy, *Anti-Corros. Methods Mater.* **1999**, *46*, 23.

[28] S. L. Li, H. Y. Ma, S. B. Lei, R. Yu, S. H. Chen, D. X. Liu, *Corrosion* **1998**, *54*, 947.

[29] K. Juttner, *Electrochim. Acta* **1990**, *35*, 1501.

[30] A. A. Ec Hosary, R. M. Saleh, A. M. Shams El Din, *Corros. Sci.* **1972**, *12*, 897.

[31] F. Mansfeld, M. W. Kendig, W. J. Lorenz, *J. Electrochem. Soc.* **1985**, *132*, 290.

[32] G. Gunasekaran, L. R. Chauhan, *Electrochim. Acta* **2004**, *49*, 4387.

[33] M. S. Morad, *Corros. Sci.* **2000**, *42*, 1307.

[34] X. Wu, H. Ma, S. Chen, Z. Xu, A. Sui, *J. Electrochem. Soc.* **1999**, *146*, 1847.

[35] W. Scheider, *J. Phys. Chem.* **1975**, *79*, 127.

[36] H. Ma, S. Chen, X. Chen, G. Li, X. Yang, *J. Serb. Chem. Soc.* **1997**, *62*, 1201.

[37] O. Olivares-Xometl, N. V. Likhanova, R. Martinez-Palou, M. A. Dominguez-Aguilar, *Mater. Corros.* **2009**, *60*, 14.

[38] M. Touzet, M. Cid, M. Puiggali, M. C. Petit, *Corros. Sci.* **1993**, *34*, 1187.

[39] D. D. Macdonald, M. C. H. Mckubre, in: J. O'. M. Bockris, B. E. Conwey, R. E. White (Eds.), *Modern Aspects of Electrochemistry*, Plenum Press, New York, 1982.

[40] A. Alagta, I. Felhosi, J. Telegdi, I. Bertoti, E. Kalman, *Corros. Sci.* **2007**, *49*, 2754.

[41] K. Babic-Samardzija, C. Lupu, N. Hackerman, A. R. Barron, A. Luttge, *Langmuir* **2005**, *21*, 12187.

[42] K. F. Khaled, *Electrochim. Acta* **2003**, *48*, 2493.

[43] E. Machnikova, K. H. Whitmire, N. Hackerman, *Electrochim. Acta* **2008**, *53*, 6024.

[44] A. Bonnel, F. Dabosi, C. Deslovis, M. Duprat, M. Keddam, B. Tribollet, *J. Electrochem. Soc.* **1983**, *130*, 753.

[45] C. T. Wang, S. H. Chen, H. Y. Ma, L. Hua, N. X. Wang, *J. Serb. Chem. Soc.* **2002**, *67*, 685.

[46] I. Felhosi, J. Telegdi, G. Palinkas, E. Kalman, *Electrochim. Acta* **2002**, *47*, 2335.

[47] J. F. Moulder, W. F. Stickle, P. E. Sobol, K. D. Bamben, *Handbook of X-Ray Photoelectron Spectroscopy: A Reference Book of Standard Spectra for Identification and Interpretation of XPS Data*, Physical Electronics, USA, **1995**.

[48] E. Kalman, F. H. Karman, I. Cserny, L. Kover, J. Telegdi, D. Varga, *Electrochim. Acta* **1994**, *39*, 1179.

[49] N. S. Mc Intyre, D. G. Zetaruk, *Anal. Chem.* **1977**, *49*, 1521.

[50] S. Maroie, M. Sally, J. J. Verbist, *Inorg. Chem.* **1979**, *18*, 2560.

[51] K. Asami, K. Hashimoto, S. Shimodaira, *Corros. Sci.* **1976**, *16*, 35.

[52] M. Koudelka, J. Sanchez, J. Augustynski, *J. Electrochem. Soc.* **1982**, *129*, 1186.

[53] B. E. Moriarty, Presented at *Corrosion 89*, New Orleans Convention Center, New Orleans, Louisiana **1989**, Paper 612.

[54] N. Nakayama, *Corros. Sci.* **2000**, *42*, 1897.

[55] N. Ochoa, G. Baril, F. Moran, N. Pebere, *J. Appl. Electrochem.* **2002**, *32*, 497.

[56] G. P. Cicileo, B. M. Rosales, Fe. Varela, J. R. Vilche, *Corros. Sci.* **1999**, *41*, 1359.

[57] K. Aramaki, T. Shimura, *Corros. Sci.* **2003**, *45*, 2639.

[58] F. H. Karman, I. Felhosi, E. Kalman, I. Cserny, L. Kover, *Electrochim. Acta* **1998**, *43*, 69.

[59] J. L. Fang, Y. Li, X. R. Ye, Z. W. Wang, Q. Liu, *Corrosion* **1993**, *49*, 266.

[60] K. Aramaki, *Corros. Sci.* **2003**, *45*, 1085.

[61] K. D. Demadis, S. Katarachia, *Phosphorus, Sulfur Silicon Relat. Elem.* **2004**, *179*, 627.

[62] N. B. Colthup, L. H. Daly, S. E. Wiberley, *Introduction to Infrared and Raman Spectroscopy*, 3rd Edn., Academic Press, New York, **1990**.

[63] K. Nakamoto, *Infrared and Raman Spectra of Inorganic and Coordination Compounds*, 4th Edn., Johnwiley & Sons, New York, **1986**.

[64] H. Amar, J. Benzakour, A. Derja, D. Villemin, B. Moreau, T. Braisaz, A. Tounsi, *Corros. Sci.* **2008**, *50*, 124.

[65] R. O. Carter,, III, C. A. Giercgak, R. A. Dickie, *Appl. Spectrosc.* **1986**, *40*, 649.

[66] K. D. Demadis, D. Coucouvanis, *Inorg. Chem.* **1995**, *34*, 436.

[67] S. Yee, G. M. Chow, *J. Mater. Chem.* **2004**, *14*, 2781.

[68] L. J. Bellamy, *Advances in Infrared Group Frequencies*, The Chaucer Press Ltd., Great Britain, **1968**, p. 94.

[69] R. Holm, D. Holtkamp, R. Kleinstuck, H.-J. Rother, S. Storp, *Fresenius Z. Anal. Chem.* **1989**, *333*, 546.

[70] J.-G. Mao, A. Clearfield, *Inorg. Chem.* **2002**, *41*, 2319.

[71] Yu. I. Kuznetsov, Presented at *The European Corrosion Congress (EUROCORR 2003)*, Budapest, Hungary **2003**, Paper 320.

[72] A. J. Freedman, *Mater. Perform.* **1984**, *23*, 9.

[73] A. Shaban, E. Kalman, I. Biczo, *Corros. Sci.* **1993**, *35*, 1463.

[74] I. Felhosi, E. Kalman, P. Poczik, *Russ. J. Electrochem.* **2002**, *38*, 230.

(Received: March 31, 2009) W5333
(Accepted: June 1, 2009)